Sigma J Eng & Nat Sci 38 (2), 2020, 589-601

Sigma Journal of Engineering and Natural Sciences
Sigma Mühendislik ve Fen Bilimleri Dergisi

Review Article

MODELING AND OPTIMIZATION OF ZINC RECOVERY FROM ENYIGBA SPHALERITE IN A BINARY SOLUTION OF ACETIC ACID AND HYDROGEN PEROXIDE

Ikechukwu A. NNANWUBE*[1], Judith N. UDEAJA[2], Okechukwu D. ONUKWULI[3]

[1]*Dept. of Chemical Engineering, Madonna University, Akpugo, NIGERIA;* ORCID: 0000-0002-0990-9566
[2]*Department of Chemical Engineering, Nnamdi Azikiwe University, Awka, NIGERIA;*
ORCID: 0000-0002-3821-1263
[3]*Department of Chemical Engineering, Nnamdi Azikiwe University, Awka, NIGERIA;*
ORCID: 0000-0002-0861-3536

Received: 24.11.2019 Revised: 23.12.2019 Accepted: 22.01.2020

ABSTRACT

This work focused on the modeling and optimization of zinc recovery from sphalerite in a binary solution of acetic acid and hydrogen peroxide. The sphalerite sample was characterized using X-ray fluorescence (XRF), X-ray diffraction (XRD) and Scanning electron micrograph (SEM). The result revealed that the ore exists as zinc sulphide (ZnS). Levenberg-Marquardt (LM) back-propagation algorithm was employed for artificial neural network (ANN) modeling while central composite rotatable design (CCRD) was deployed for response surface methodology (RSM) modeling. RSM modeling gave optimum conditions of 90^{o}C leaching temperature, 6M acid concentration, 540 rpm stirring rate, 120 minutes leaching time and 6M hydrogen peroxide concentration; at which about 89.91% zinc was recovered. Comparison of the two modeling techniques revealed that ANN (root mean square error, RMSE = 0.530, absolute average deviation, AAD = 0.681, coefficient of determination = 0.996) gave better predictions than RSM (root mean square error, RMSE = 0.755, absolute average deviation, AAD = 0.841, coefficient of determination = 0.991). Hence, ANN demonstrated higher predictive capability than RSM.
Keywords: Sphalerite, acetic acid, hydrogen peroxide, optimization, artificial neural network, response surface methodology.

1. INTRODUCTION

For several decades, a number of processes have been developed to leach sulphide ores and concentrates and the conditions are well established. However, there is a renewed interest in hydrometallurgical processes for zinc production from sphalerite (ZnS) due to environmental issues and the increasing need to exploit mixed and low grade ores and relatively small deposits [1].

Sphalerite is considered to be the most important zinc sulphide mineral and is of economic importance. It is found in metamorphic, igneous and sedimentary rocks in many parts of the

* Corresponding Author: e-mail: ik.nnanwube@gmail.com, tel: +2347033164674

world. It is normally associ ated with other sulphide minerals such as galena (PbS), pyrite (FeS_2), chalcopyrite ($CuFeS_2$) and barite ($BaSO_4$) [2].

Zinc has found many applications as catalyst in organic synthesis including asymmetric synthesis, being cheap and easily available alternative to precious metal complexes [3]. A variety of zinc compounds are used industrially. Zinc oxide is widely used as a white pigment in paints, and as a catalyst in the manufacture of rubber. It is also used as a heat disperser for the rubber and acts to protect its polymers from ultraviolet radiation ([4].

The leaching of sulphide minerals requires high oxidation potential. This challenge can be overcome by leaching with oxidative reagent such as hydrogen peroxide [2]. Hence, in the present investigation, the synergistic effect of a binary solution of acetic acid and hydrogen peroxide as a leachant for zinc recovery from sphalerite is investigated. Sphalerite releases zinc ion in acidic medium and forms the elemental sulphur as shown in Equation (1).

$$ZnS_{(s)} \longrightarrow Zn^{2+}_{(aq)} + S^{o}_{(s)} + 2e^{-} \quad (1)$$

The leaching of sphalerite in a binary solution of acetic acid and hydrogen peroxide is illustrated in Equation (2).

$$ZnS_{(s)} + H_2O_{2(aq)} + 2H^{+}_{(aq)} \longrightarrow Zn^{2+}_{(aq)} + S^{o}_{(s)} + 2H_2O_{(l)} \quad (2)$$

The traditional method of studying a process by changing one variable at a time and keeping the other variables at a constant level does not depict the combined effect of all the factors involved. In addition, the traditional methods have been reported to be laborious, with low efficiency, low recovery rate of target components, excessive consumption of solvents, energy and time [5].

Response surface methodology (RSM) is an advanced statistical and mathematical method used for process improvement and optimization [6]. Its main objective is to determine optimum operational conditions for a given system or process. The application of statistical experimental design techniques in leaching process can lead to improved product yield, reduced processing time and overall costs [7]. On the other hand, artificial neural networks can be viewed as non-linear regression tool for making a relationship between input and output variables. Generally, a neural network contains one input layer, one or more hidden layers, and one output layer [8]. They are the most popular artificial learning tool with a wide applications range, which include biodiesel production [5, 9], fluid extraction [10], wastewater treatment [11], metal recovery [8, 12], et. cetera.

The modeling and optimization of sphalerite dissolution in acid solution had been reported [13]. However, there is no reported work known to the authors on the application of artificial neural network in modeling the process. The present investigation focused at optimizing process variables viz. acetic acid concentration, hydrogen peroxide concentration, stirring rate, leaching temperature and leaching time for optimum zinc recovery using RSM. A comparison of the two modeling techniques was also carried out.

2. MATERIAL AND METHODS

2.1. Materials

Sphalerite sample used in this study was obtained from Enyigba mining site, in Ebonyi state of Nigeria. The ore sample was pulverized and sieved with 75µm sieve. Analytical grade reagents and deionized water were used to prepare all solutions.

2.2. Analytical methods

The chemical composition of the ore was determined with X-ray fluorescence spectroscopy (XRF) via X-supreme 60 oxford instruments. The mineralogical composition of the ore sample

was determined with X-ray diffraction (XRD) with ARL X'TRA X-ray Diffractometer, Thermoscientific with the serial number 197492086 using Cu Kα radiation at 45kV and 40mA. The XRD patterns were recorded in the range of 5-65^o 2θ. Scanning electron microscopy (SEM) Q250 by FEI model was used to perform the SEM analysis.

2.3. Leaching procedure

The leaching experiments were performed in a 500 ml flat-bottomed flask. The flask was fitted with a condenser to prevent losses through evaporation. A magnetically-stirred hot plate was used to provide heating. The calculated volumes of CH_3COOH and H_2O_2 solutions were added to the flask, which was then heated to the desired temperature. Subsequently, a sample with a pre-determined weight was added to the flask. At the completion of each reaction time, the undissolved materials in the suspension was allowed to settle and separated by filtration. The resulting solutions were diluted and analyzed for zinc using atomic absorption spectrophotometer (AAS) [4].

2.4. XRF analysis description

About 20g of the ore sample was dried and sieved through 2mm sieves. Samples were milled further to between 20-53 μm. About 5g homogeneous specimen of the sample was loaded into special XRF cups prepared with 4μm ultralene film. The cups were half-full with sample. The instrument was switched on and taken to measurement mode. The measurement software was opened and the desired method selected. The sample was placed on the instrument in its bench top measurement position setup and covered. The sample compartment lid was closed to prevent scattering X-ray radiation. The measurement conditions as well as the time for each condition were set. The sample details were entered. The trigger was pulled to start the measurement. All detectable elements were measured simultaneously. Raw qualitative spectra and quantified result were stored in the software.

2.5. Design of experiment for RSM modeling

A five-level-five-factor CCRD was employed in the modeling and optimization studies, which produced 32 experimental runs. The independent factors chosen for the optimization include leaching temperature, acid concentration, stirring rate, leaching time and hydrogen peroxide concentration. The response variable was chosen as % yield of zinc. The coded and uncoded levels of the independent factors are shown in Table 1. Experiments were performed according to the actual experimental design matrix shown in Table 2. The experiments were performed randomly to avoid systemic error. In order to correlate the response variable to the independent variables, multiple regressions were used to fit the coefficient of the second-order polynomial model of the response. The quality of the fit of the model was evaluated using a test of significance and analysis of variance (ANOVA). In RSM, the most widely used second-order polynomial equation developed to fit the experimental data and identify the relevant model terms is shown in Equation 3.

$$Y = \beta_0 + \sum_{i=1}^{n} \beta_i x_i + \sum_{\substack{i=1 \\ j>1}}^{n-1} \sum_{j=2}^{n} \beta_{ij} x_i x_j + \sum_{i=1}^{n} \beta_{ii} x_i^2 + \varepsilon \quad (3)$$

where Y is the predicted response variable which is the % yield of zinc in this study, β_0 is the constant coefficient, β_i is the ith linear coefficient of the input variable x_i, β_{ii} is the ith quadratic coefficient of the input variable x_i, β_{ij} is the different interaction coefficients between the input

variables x_i and x_j and ε is the error of the model. Design Expert software package version 10.0 (Stat-Ease Inc., Minneapolis, MN, USA) was used for regression analysis and analysis of variance (ANOVA).

Table 1. Experimental range of the independent variables with different levels, to study sphalerite dissolution in a binary solution of acetic acid (CH_3COOH) and hydrogen peroxide (H_2O_2)

Independent variable	Unit	Symbol	Coded variable levels				
			-α	-1	0	+1	-α
Leaching temperature	^oC	X_1	45	60	75	90	105
Acid concentration	M	X_2	0.75	2.5	4.25	6.0	7.75
Stirring rate	rpm	X_3	75	230	385	540	695
Leaching time	min	X_4	30	60	90	120	150
Hydrogen Peroxide	M	X_5	0.75	2.5	4.25	6.0	7.75

Table 2. Experimental design matrix for sphalerite dissolution in a binary solution of acetic acid (CH_3COOH) and hydrogen peroxide (H_2O_2)

Run	A:Leaching temp.		B:Acid conc.		C:Stirring rate		D:Leaching time		E:Hydrogen Peroxide	
	Coded	Real	Coded	Real	Coded	Real	Coded	Real	Coded	Real
1	-1	60	+1	6	-1	230	-1	60	-1	2.5
2	+1	90	+1	6	+1	540	-1	60	-1	2.5
3	-2	45	0	4.25	0	385	0	90	0	4.25
4	0	75	0	4.25	0	385	0	90	0	4.25
5	0	75	0	4.25	+2	695	0	90	0	4.25
6	0	75	0	4.25	0	385	0	90	+2	7.75
7	0	75	0	4.25	0	385	0	90	0	4.25
8	-1	60	+1	6	-1	230	+1	120	+1	6
9	+1	90	-1	2.5	+1	540	-1	60	+1	6
10	0	75	-2	0.75	0	385	0	90	0	4.25
11	-1	60	-1	2.5	-1	230	+1	120	-1	2.5
12	+1	90	+1	6	-1	230	-1	60	+1	6
13	+1	90	-1	2.5	+1	540	+1	120	-1	2.5
14	+1	90	+1	6	-1	230	+1	120	-1	2.5
15	-1	60	-1	2.5	+1	540	+1	120	+1	6
16	0	75	0	4.25	0	385	0	90	0	4.25
17	-1	60	-1	2.5	-1	230	-1	60	+1	6
18	+2	105	0	4.25	0	385	0	90	0	4.25
19	0	75	0	4.25	0	385	-2	30	0	4.25
20	0	75	0	4.25	0	385	+2	150	0	4.25
21	-1	60	+1	6	+1	540	+1	120	-1	2.5
22	0	75	0	4.25	0	385	0	90	0	4.25
23	0	75	0	4.25	0	385	0	90	-2	0.75
24	0	75	0	4.25	0	385	0	90	0	4.25
25	-1	60	+1	6	+1	540	-1	60	+1	6
26	+1	90	+1	6	+1	540	+1	120	+1	6
27	0	75	+2	7.75	0	385	0	90	0	4.25
28	0	75	0	4.25	0	385	0	90	0	4.25
29	-1	60	-1	2.5	+1	540	-1	60	-1	2.5
30	0	75	0	4.25	-2	75	0	90	0	4.25
31	+1	90	-1	2.5	-1	230	+1	120	+1	6
32	+1	90	-1	2.5	-1	230	-1	60	-1	2.5

3. RESULTS AND DISCUSSION

3.1. Characterization

The results of the XRF analysis of the sphalerite sample had earlier been reported [4]. The result as shown in Figure 1 revealed that ZnO, SO_3, Na_2O and Fe_2O_3 were the major oxides present in the ore; oxides such as SiO_2, CaO, Al_2O_3, Mn_2O_3 and MgO were present in minor quantities while the rest occurred in traces.

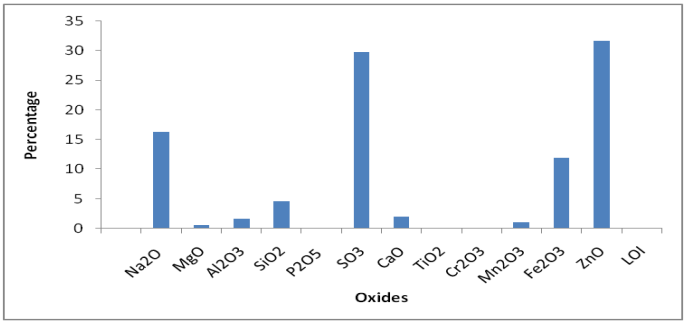

Figure 1. XRF result of Enyigba sphalerite

The XRD result revealed the presence of sphalerite (ZnS) as the dominant mineral with three major peaks at 28.56, 47.50 and 56.37^o, respectively. The result also revealed the presence of cerium germanium sulphide (Ce_2GeS_2) as an associated mineral with three major peaks at 30.15, 43.16 and 26.03^o, respectively, as shown in Figure 2 [4].

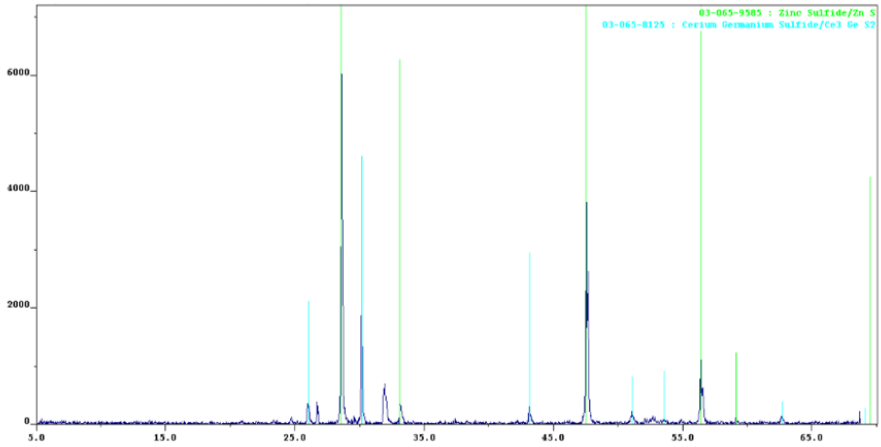

Figure 2. X-ray diffraction pattern of Enyigba sphalerite

The scanning electron micrograph (SEM) of sphalerite is presented in Figure 3 with magnifications of 500x, 1000x and 1500x, respectively. The results indicate that the particles are very cohesive, confirming their micrometer sized agglomerates with irregular shapes and rough edges and form microscopic flakes. The particles are highly crystalline, indicating a high level of purity of the ore.

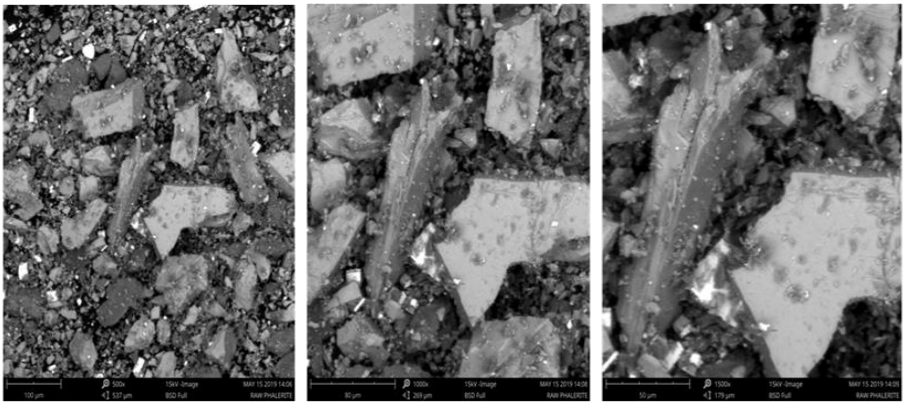

(a) (b) (c)

Figure 3. SEM images of Enyigba sphalerite showing magnifications of 500× (a), 1000× (b) and 1500× (c), respectively.

3.2. RSM modeling

The analysis of the experimental results presented in Table 2 was done using design expert software (Design Expert 10.0). Models analyzed include: Linear model, 2FI (two factors interaction), quadratic and cubic model. Model quality (goodness of fit) can be compared based on the model's R^2 values and other parameters such as standard deviation (SD), prediction error sum of squares (PRESS), R^2 adjusted, R^2 predicted, model's F-value and P-values. The closer the R^2 value to unity, the better the models fit (Ameer et al., 2017b). From the model analyses presented as model summary statistics in Table 3, quadratic model with the highest regression coefficient (R^2 value of 0.9913), least standard deviation of 1.29 shows better correlation between the observed and model predicted data. The PRESS is a measure of how well the model is likely to predict the responses in a new experiment. Low PRESS shows model's reliability for predicting responses. The low PRESS value of 349.04 suggests that the quadratic model described the experimental design responses better than other models (Linear, 2FI and cubic), with the cubic model being aliased. In addition, a model is accepted as adequate if the difference between the adjusted R-Squared and the predicted R-Squared is less than 0.2. From Table 3, quadratic model has the least difference between Adjusted R^2 and Predicted R^2 of 0.1423. Hence, it can be inferred that the suggested model is adequate.

Table 3. Model summary statistics

Source	Standard Deviation	R^2	Adjusted R^2	Predicted R^2	PRESS	Remarks
Linear	4.83	0.7094	0.6536	0.6362	761.07	
2FI	6.03	0.7220	0.4614	-2.5942	7518.70	
Quadratic	1.29	0.9913	0.9754	0.8331	349.04	Suggested
Cubic	0.96	0.9973	0.9863	0.9901	20.67	Aliased

The in-depth analysis of the fitness of the selected model (quadratic) was done using analysis of variance (ANOVA). The model's statistical parameters such as model's P-Value, degrees of freedom (df), Lack of Fit (LOF), coefficient of determination (R^2), coefficient of variation (C.V), and signal to noise ratio (S/N) were computed. The model's ANOVA results are presented in Table 4.

Table 4. ANOVA for response surface quadratic model

Source	Coefficient Estimate	Sum of Squares	Degree of Freedom	F-value	P-value (Prob > F)
Model	87.12	2073.63	20	62.47	< 0.0001
X_1	3.42	*280.85*	*1*	*169.22*	*< 0.0001*
X_2	3.73	*333.76*	*1*	*201.10*	*< 0.0001*
X_3	3.23	*250.26*	*1*	*150.79*	*< 0.0001*
X_4	3.58	*307.45*	*1*	*185.25*	*< 0.0001*
X_5	3.60	*311.76*	*1*	*187.85*	*< 0.0001*
X_1X_2	-0.54	*4.73*	*1*	*2.85*	*0.1195*
X_1X_3	-0.21	*0.68*	*1*	*0.41*	*0.5350*
X_1X_4	-0.081	*0.11*	*1*	*0.064*	*0.8055*
X_1X_5	-0.34	*1.89*	*1*	*1.14*	*0.3087*
X_2X_3	-0.67	*7.16*	*1*	*4.31*	*0.0621*
X_2X_4	-0.32	*1.63*	*1*	*0.98*	*0.3436*
X_2X_5	-0.43	*2.98*	*1*	*1.79*	*0.2076*
X_3X_4	-0.056	*0.051*	*1*	*0.031*	*0.8645*
X_3X_5	-0.34	*1.89*	*1*	*1.14*	*0.3087*
X_4X_5	-0.57	*5.18*	*1*	*3.12*	*0.1051*
X_1^2	-2.41	*170.56*	*1*	*102.77*	*< 0.0001*
X_2^2	-2.49	*181.34*	*1*	*109.26*	*< 0.0001*
X_3^2	-1.82	*97.58*	*1*	*58.79*	*< 0.0001*
X_4^2	-2.37	*165.30*	*1*	*99.60*	*< 0.0001*
X_5^2	-2.12	*132.32*	*1*	*79.73*	*< 0.0001*
Residual		18.26	11		
Lack of fit		*12.72*	*6*	*1.92*	*0.2462*
Pure error		*5.53*	*5*		
Cor. Total		2091.89	31		

The adequacy or significance of the selected model (quadratic) was confirmed based on the model's F-value. A model is significant at the 95% confidence level if the Fisher test (F-test) has a probability value (Prob>F) below 0.05. From table 4, it was observed that the model's F-test has a probability value (Prob>F) of 0.0001 which is below 0.05.

The lack of fit (LOF) F-test describes the deviation of actual points from the fitted surface, relative to pure error. It shows the fitness of the individual data points to the suggested model. A large value of Prob>F for LOF, possibly greater than 0.05, is preferred. The LOF P-value of 0.2462 (non-significant) was obtained indicating that there is significant effect of process variables on the output response.

The ANOVA coefficient of variation (CV) is the ratio of the standard error to the mean value of the observed response. It measures reproducibility of the model. A model can be considered reasonable if its CV is less than 15%. From the summary of regression table (Table 5) the overall average of response data (mean) was found to be 78.71 while 1.64% was obtained as the C.V. This result confirms that the suggested model (quadratic) is reasonable and reproducible.

Table 5. Summary of regression values

Std. Dev.	Mean	C.V. %	PRESS	Adeq. Precision
1.29	78.71	1.64	349.04	25.025

Adequate precision (AP) measures the experimental signal to noise ratio, it indicates the model adequacy in making predictions. A model shows reasonable performance in prediction if it

has an AP greater than 4. From the present study, Adequate Precision ratio of 25.025 was obtained (Table 5) indicating that the model equation can be used for response prediction.

The regression model formulated by the design expert, relating responses and variables in terms of coded factors after eliminating the statistically insignificant terms is shown in Equation 4. The actual significant model obtained after eliminating the insignificant model terms is presented in Equation 5.

$$\text{Yield} = 84.12 + 3.42X_1 + 3.73X_2 + 3.23X_3 + 3.58X_4 + 3.60X_5 - 2.41X_1^2 - 2.49X_2^2 - 1.82X_3^2 - 2.37X_4^2 - 2.12X_5^2 \quad (4)$$

Yield = -116.73 + 2.03 * Leaching temperature + 12.68 * Acid concentration + 0.10 * Stirring rate + 0.68 * leaching time + 11.00* Hydrogen Peroxide conc. – 0.01 * Leaching temp.^{2} – 0.81 * Acid concentration^2 – 7.59E-005 * Stirring rate^2 - 2.64E-003 * Leaching time^2 – 0.69 * Hydrogen Peroxide conc.^{2} (5)

The plot of predicted vs actual values show the effect of the model (by providing a visual assessment of model fit). In addition, it compares the predicted data points with the actual experimental data. From Figure 4, the data points are aligned along a straight diagonal, which is an indication of high correlation between the actual values and model predicted values.

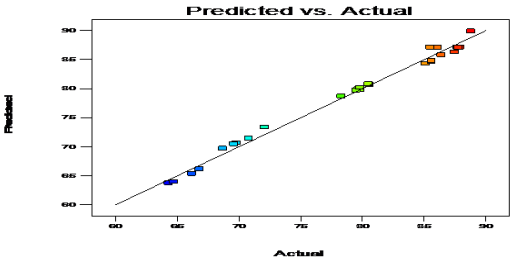

Figure 4. Plot of Model Predicted vs Actual values

3.3. Response surface plots

The three-dimensional response surface plots, obtained as a function of two factors while maintaining all the factors constant at the mid-values, are helpful in understanding both the main effects and the interaction effects of these five factors. The model equations were solved for the various interaction effects on zinc yield considering at any instance the interaction between two factors only, assuming the other variables are set at their mean coded value of zero (0). The combined effects of adjusting the process variables within the design space were monitored using the 3D surface plots. Figure 5a shows the effects of leaching temperature and acid concentration on the percentage zinc yield. As the leaching temperature increased from 66 to 84^{o}C, the percentage yield of zinc increased from 85 to 88.5%; while the percentage zinc yield also increased by the same margin as the acid concentration increased from 3.2 to 5.3M. The interactive effect of stirring rate and leaching temperature is shown in Figure 5b. As the stirring rate increased from 230 to 540 rpm, the percentage yield of zinc increased from 83 to 89.5%; whereas as the leaching temperature increased from 60 to 84^{o}C, the percentage yield of zinc increased from 82.5 to 90%. Figure 5c shows the interactive effect of leaching time and leaching temperature. As the leaching temperature increased from 60 to 84^{o}C, the percentage recovery of zinc increased from 82.5 to 90%; while the percentage recovery of zinc also increased by the same margin as the leaching time increased from 60 to 110 minutes. The combined interactive effect of leaching temperature and hydrogen peroxide concentration is given in Figure 5d. As the leaching temperature increased from 60 to 84^{o}C, the percentage yield of zinc increased from 82.5

to 90%; whereas as the hydrogen peroxide concentration increased from 2.5 to 5.3M, the percentage recovery of zinc increased from 83 to 89.5%.

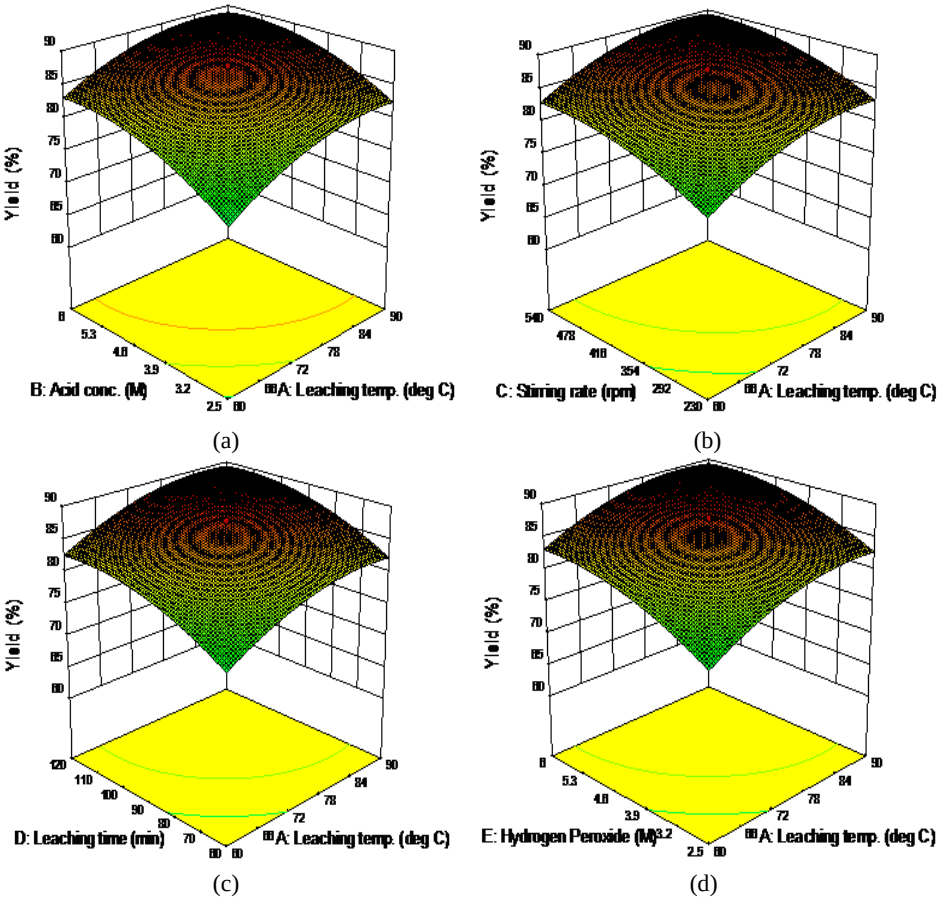

Figure 5. 3D plots of effects of process variables on zinc recovery

3.4. ANN modeling

In the present study, a three-layered feed-forward neural network with tangent sigmoid transfer function (tansig) at the hidden layer and linear transfer function (purelin) at the output layer was used. The model developed was used for the prediction of zinc yield. The ANN was trained using the back propagation algorithm. All calculations were carried out with MATLAB R2007b software (The mathworks, Inc., Ver. 7.5.0.342, MA, USA). This architecture was manipulated by modifying the number of neurons in the hidden layer. The topology of the developed ANN model was assigned as 5-9-1, where the 5 neurons of layer 1 correspond to the 5 input variables (leaching temperature, acid concentration, stirring rate, leaching time and hydrogen peroxide concentration); the hidden layer has 9 neurons while the output layer has one neuron, representing the target response (zinc yield). The same experimental dataset employed for RSM modeling was used for simulation by the ANN. During the training process, the whole experimental dataset (32 runs) was divided into 3 subsets, with a proportion of approximately

70:20:10 (%) for training, validation, and testing. The splitting of the dataset into different subsets allows evaluation of the predictive performance of the neural network with respect to the "hidden" data that is not used for the training purposes [14]. The network architecture was evaluated to achieve the lowest possible training, validation and testing errors and highest correlation coefficients. From the results obtained, the mean square error of the trained network is 8.06709e-1 with a regression coefficient of 0.997755. The performance plot for the trained network is shown in Figure 6 with 6 epochs while the regression plots for the training and validation are shown in Figure 7 (a and b).

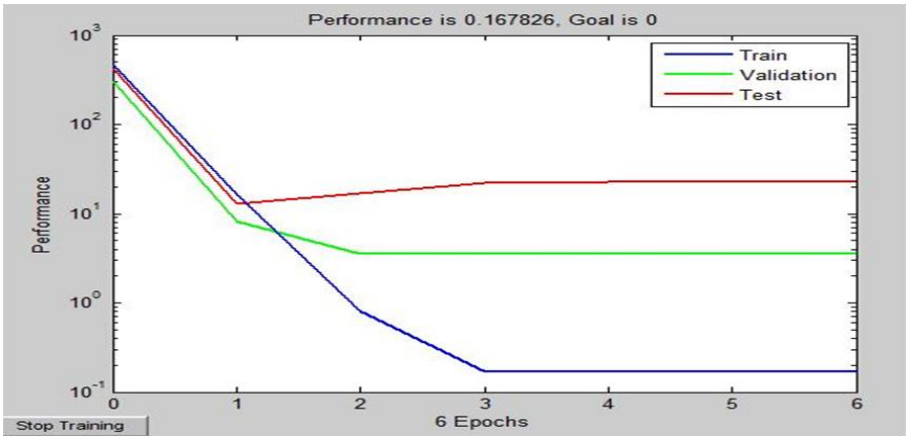

Figure 6. Performance plot for sphalerite dissolution in CH_3COOH/H_2O_2 ANN model

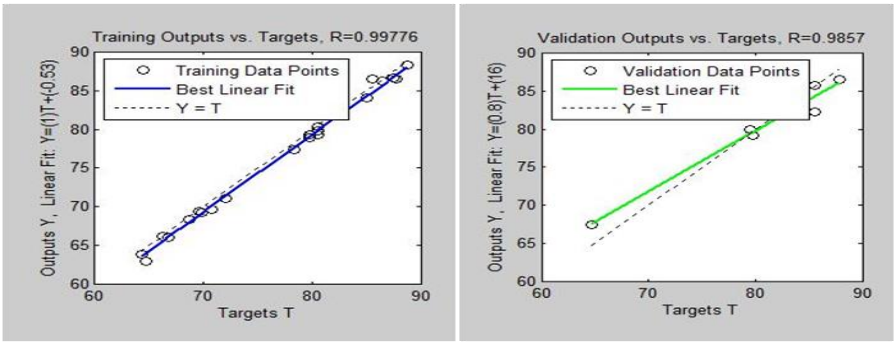

(a) (b)

Figure 7. Regression plots for the training (a) and validation (b) for sphalerite dissolution in CH_3COOH/H_2O_2

3.5. Performance evaluation of RSM and ANN models

A comparative study between artificial neural network (ANN) and response surface methodology (RSM) was carried out in order to assess the respective predictive performance and estimation capabilities by means of various statistical indicators, including root mean square error (RMSE), absolute average deviation (AAD), mean absolute error (MAE), coefficient of determination (R^2), and standard error of prediction (SEP) observed for both models. The closer the RMSE and MAE values are to 0, the better the prediction of the model. The RMSE was

calculated using Equation (6). The AAD observed for both models gives an indication of how accurate the model predictions can be [15]. The lower the AAD (%) value, the better the prediction of the model. Equation (7) shows the expression for calculating the absolute average deviation (AAD); the expression for calculating the coefficient of determination (R^2), is shown in Equation (8); while the expressions for calculating the mean absolute error (MAE) and the standard error of prediction (SEP) are shown in Equations (9) and (10), respectively.

$$\text{RMSE} = \left(\frac{1}{n} \sum_{i=1}^{n} \left(Y_{pred.} - Y_{\exp.} \right)^2 \right)^{\frac{1}{2}} \tag{6}$$

$$\text{AAD (\%)} = \left(\frac{1}{n} \sum_{i=1}^{n} \left\{ \frac{\left| Y_{pred.} - Y_{\exp.} \right|}{Y_{\exp.}} \right\} \right) \times 100 \tag{7}$$

$$R^2 = 1 - \frac{\sum_{i=1}^{n} \left(Y_{\exp.,i} - Y_{pred.,i} \right)^2}{\sum_{i=1}^{n} \left(Y_{\exp.,i} - Y_{\exp.,ave} \right)^2} \tag{8}$$

$$MAE = \frac{1}{n} \sum_{i=1}^{n} \left| \left(Y_{\exp.,i} - Y_{pred.,i} \right) \right| \tag{9}$$

$$SEP = \frac{RMSE}{Y_{\exp.,ave}} \times 100 \tag{10}$$

where n is the number of sample points, $Y_{pred.}$ is the predicted response value of zinc dissolution and $Y_{exp.}$ is the experimentally determined value for zinc dissolution [15].

The results of the statistical comparison between RSM and ANN models are presented in Table 6. The value of R^2 for the ANN model was slightly higher than the value for RSM model. Also, the computed values of RMSE, AAD, MAE and SEP for both models were very low. AAD was used to measure the precision and accuracy of the models. The values obtained for both models were very low. However, the ANN model had lower error values than the RSM model, suggesting the superiority of ANN over RSM for predictability purpose.

Table 6. Predicive capacity comparison of RSM and ANN models

Parameters	Yield (%)	
	RSM	ANN
RMSE	0.755	0.530
AAD (%)	0.841	0.681
R^2	0.991	0.996
MAE	0.654	0.530
SEP	0.959	0.673

3.6. Process optimization using CCD

The optimization exercise for the dissolution process was conducted independently using the pliability of the design expert tool. Equation 3 was solved for the best solutions such that the response was maximized within the design space. A conventional approach, which involves selecting the best solution based on economic considerations, was adopted. The optimal predicted conditions for zinc recovery include a leaching temperature of 90^{o}C, acid concentration of 6M, stirring rate of 540 rpm, leaching time of 120 minutes and hydrogen peroxide concentration of 6M; at which about 89.91% zinc was recovered. Experiments were performed in triplicate at the above optimum conditions to validate the RSM predicted result. An average value of 88.47% zinc recovery was recorded.

4. CONCLUSION

In this work, the potential of a binary solution of acetic acid and hydrogen peroxide as a lixiviant for the recovery of zinc from sphalerite was investigated. Characterization of the sphalerite mineral showed that it exists as zinc sulphide. The central composite rotatable (CCRD) was deployed for the RSM modeling while Levenberg-Marquardt (LM) back propagation (BP) algorithm was deployed for ANN modeling. Optimum predicted conditions from RSM modeling include a leaching temperature of 90^{o}C, acid concentration of 6M, stirring rate of 540 rpm, leaching time of 120 minutes and hydrogen peroxide concentration of 6M; at which about 89.91% zinc was recovered. The two modeling techniques were compared using statistical indicators such as RMSE, AAD, R^2, MAE and SEP. The results revealed that ANN gave better predictions than RSM.

Acknowledgements

The authors acknowledge the national research institute for chemical technology (NARICT), Kaduna, Nigeria, for performing the XRF, XRD and SEM analyses.

REFERENCES

[1] Nwoye C. I., Nwabanne J. T., Odo J. U., (2013) Open System Leaching of Sphalerite in Butanoic Acid Solution and Empirical Analysis of Zinc Extraction Based on Initial Solution pH, Leaching Time and Mass-Input, *Research Journal of Chemical Sciences*, 3(5), 25-31.

[2] Hasani M., Koleini S. M. J., Khodadadi A., (2016) Kinetics of Sphalerite Leaching by Sodium Nitrate in Sulphuric Acid, *Journal of Mining and Environment, 7(1), 1–12.*

[3] Lowicki D., Bas S., Mlynarski J., (2015) Chiral Zinc Catalysts for Asymmetric Synthesis, *Tetrahedron, 71(9), 1339-1394.*

[4] Onukwuli O. D., Nnanwube I. A., (2018) Hydrometallurgical Processing of a Nigerian Sphalerite Ore in Nitric Acid: Characterization and Dissolution Kinetics. *The International Journal of Science and Technoledge, 6(3), 40-54.*

[5] Betiku E., Okunsolawo S. S., Ajala S. O., Odelede O. S., (2015) Performance Evaluation of Artificial Neural Network Coupled with Genetic Algorithm and Response Surface Methodology in Modeling and Optimization of Biodiesel Production Process Parameters From Shea Tree (Vitellaria Paradoxa) Nut Butter, *Renewable Energy, 76, 408 – 417.*

[6] Ameer K., Bae S. W., Jo Y., Lee H. G., Ameer A., Kwon J. H., (2017a). Optimization of Microwave-Assisted Extraction of Total Extract, Stevioside and Rebaudioside-A From Stevia Rebaudiana (Bertoni) Leaves Using Response Surface Methodology (RSM) and Artificial Neural Network (ANN) Modeling, *Food Chemistry,* 229, 198 – 207.

[7] Ponnusamy S. K., Subramaniam R., (2013) Process Optimization Studies of Congo Red Dye Adsorption onto Cashew Nut Shell Using Response Surface Methodology, *International Journal of Industrial Chemistry, 4(17), 1-10.*

[8] Chelgani S. C., Jorjani E., (2009) Artificial Neural Network Prediction of Al_2O_3 Leaching Recovery in the Bayer Process-Jajarm Alumina Plant (Iran), *Hydrometallurgy, 97, 105-110.*

[9] Esonye C., Onukwuli O. D., Ofoefule A. U., (2019) Optimization of Methyl Ester Production from Prunus Amygdalus Seed Oil Using Response Surface Methodology and Artificial Neural Networks, *Renewable Energy, 130, 61-72*.

[10] Ameer K., Chun B., Kwon J., (2017b). Optimization of Supercritical Fluid Extraction of Steviol Glycosides and Total Phenolic Content from Stevia Rebaudiana (Bertoni) Leaves Using Response Surface Methodology and Artificial Neural Network, *Industrial Crops and Products, 109, 672 -685.*

[11] Yetilmezsoy K., Demirel S., (2008). Artificial Neural Network (ANN) Approach for Modeling of Pb (III) Adsorption from Aqueous Solution by Antep Pistachio (Pistacia Vera L.) Shells, *Journal of Hazardous Materials, 153, 1288 – 1300.*

[12] Nnanwube I. A., Onukwuli O., D., Ajana S. U., (2018). Modeling and Optimization of Galena Dissolution in Hydrochloric Acid: Comparison of Central Composite Design and Artificial Neural Network, *Journal of Minerals and Materials Characterization and Engineering, 6, 294-315.*

[13] Guler E., (2015). Pressure Acid Leaching of Sphalerite Concentrate: Modeling and Optimization by Response Surface Methodology, *Physicochemical Problems of Mineral Processing, 52(1),479-496.*

[14] Xi J., Xue Y., Xu Y., Shen Y., (2013). Artificial Neural Network Modeling and Optimization of Ultrahigh Pressure Extraction of Green Tea Polyphenols, *Food Chemistry, 141, 320-326.*

[15] Pilkington J., Preston C., Gomes R. L., (2014). Comparison of Response Surface Methodology (RSM) and Artificial Neural Network (ANN) Towards Efficient Extraction of Artemisinin from Artemisia Annua, *Industrial Crops and Products*, 58, 15 – 24.